

Mach–Zehnder Interferometer

Juan Pablo Solís Ruiz^{a,1}

^aA01067387

Professors Adad Yepiz Escalante and Rodolfo Rodríguez y Masegosa

Abstract—In this laboratory practice, a Mach–Zehnder interferometer was built and analyzed to study optical interference and related optical phenomena. We investigated the formation of interference fringes, modifications to the interferometer arms, the behavior under changes in optical path and polarization, and the influence of filters on intensity and fringe patterns. The interferometer's high sensitivity to environmental changes was highlighted, together with the relationship between field displacement and fringe orientation. These results emphasize the versatility of the Mach–Zehnder interferometer in the study of optical phenomena, underscoring the importance of considering different experimental variables to obtain precise and meaningful results in optical research.

Keywords—Mach–Zehnder Interferometer, Light Polarization, Optical Interference, Optical Phenomena, Interferometric Sensitivity

Contents

1	Introduction	1
2	Theoretical Background	1
2.1	Interference and superposition of light	1
2.2	Fresnel–Arago laws	1
2.3	Mach–Zehnder interferometer	1
2.4	Materials	2
3	Procedure	2
3.1	Interference behavior	2
3.2	Filter behavior	3
3.3	Optical path and wavefront study	3
3.4	Polarization study	4
4	Analysis and Observations	4
4.1	Interferometer behavior	4
	Interference formation and fringes • Temperature influence • Optical-path influence	
4.2	Modifications to the interferometer arms	5
	Attenuation with filters • Polarization • Wavefront modification	
5	Conclusions	5
6	Appendices	6
7	References	6

1. Introduction

In the context of optical experimentation, the Mach–Zehnder interferometer stands out as a fundamental tool for studying interference and the superposition of light. This practice focuses on exploring key optical phenomena associated with this device, from the formation of interference patterns to the influence of light polarization and interferometric sensitivity. By employing the Mach–Zehnder interferometer, we investigated the Fresnel–Arago laws, wavefront modification, and the behavior under changes in the optical path, among other aspects. This report details the experimental process, data analysis, and the observations obtained, highlighting the relevance of these investigations in the field of experimental optics and interferometric phenomena.

2. Theoretical Background

2.1. Interference and superposition of light

Thomas Young (born June 13, 1773, in Milverton, Somerset, England; died May 10, 1829, in London) was an English physician and physicist

who established the principle of interference of light and thereby revived the centuries-old wave theory of light.

According to the Superposition Principle, the intensity of the electric field E at a point in space, generated by separate fields E_1, E_2, \dots from various contributing sources, is expressed as:

$$E = E_1 + E_2 + \dots \quad (1)$$

Let us consider only linearly polarized waves of the form:

$$E_1(\mathbf{r}, t) = E_{01} \cos(\mathbf{k}_1 \cdot \mathbf{r} - vt + \epsilon_1) \quad (9.2a)$$

$$E_2(\mathbf{r}, t) = E_{02} \cos(\mathbf{k}_2 \cdot \mathbf{r} - vt + \epsilon_2) \quad (9.2b)$$

The irradiance at the observation point P is computed as:

$$I = P\langle E^2 \rangle T \quad (4)$$

For our analysis, we will ignore constants and consider:

$$I = 8\langle E^2 \rangle T \quad (5)$$

where $8\langle E^2 \rangle T$ represents the time average of the squared magnitude of the electric-field intensity.

Interference occurs when fields E_1 and E_2 overlap, producing a total irradiance given by:

$$I = I_1 + I_2 + I_{12} \quad (6)$$

where:

$$I_1 = 8\langle E_1^2 \rangle T \quad (9.5)$$

$$I_2 = 8\langle E_2^2 \rangle T \quad (9.6)$$

$$I_{12} = 2\langle E_1 \cdot E_2 \rangle T \quad (9.7)$$

The term I_{12} is known as the interference term. To evaluate it, we multiply and average:

$$E_1 \cdot E_2 = E_{01} \cdot E_{02} \cos(\mathbf{k}_1 \cdot \mathbf{r} + \epsilon_1 - \mathbf{k}_2 \cdot \mathbf{r} - \epsilon_2) \quad (10)$$

After averaging, we obtain:

$$8\langle E_1 \cdot E_2 \rangle T = \frac{1}{2} E_{01} \cdot E_{02} \cos(d) \quad (9.11)$$

where $d = (\mathbf{k}_1 \cdot \mathbf{r} - \mathbf{k}_2 \cdot \mathbf{r} + \epsilon_1 - \epsilon_2)$ represents the phase difference. If E_{01} and E_{02} are perpendicular, $I_{12} = 0$ and $I = I_1 + I_2$. When E_{01} is parallel to E_{02} , the irradiance reduces to:

$$I_{12} = 2\langle I_1 \rangle \langle I_2 \rangle \cos(d) \quad (12)$$

yielding the total irradiance:

$$I = I_1 + I_2 + 2\langle I_1 \rangle \langle I_2 \rangle \cos(d) \quad (9.14)$$

Depending on d , the resulting irradiance may be greater than, less than, or equal to $I_1 + I_2$.

2.2. Fresnel–Arago laws

More than 200 years ago, Fresnel and Arago published the laws describing the interference of polarized light. These laws were formulated from a series of experimental arrangements producing interference between polarized light beams. The experiments essentially involved observing interference fringes in Young's double-slit experiment (or variations thereof) while using polarizing optical elements along the ray paths. Their manuscript, published long before the electromagnetic theory of light was proposed, concludes with five empirical laws, stated as follows:

1. Under the same circumstances in which two rays of ordinary light appear to destroy each other, two rays polarized in opposite directions do not exert any appreciable action upon each other.
2. Rays polarized in a single direction act upon each other like natural (ordinary) rays; therefore, in these two types of light, interference phenomena are absolutely identical.
3. Two rays originally polarized in opposite directions can subsequently be brought into the same plane of polarization; however, this does not confer upon them the ability to influence each other.
4. Two rays polarized in opposite directions and subsequently brought into analogous polarizations influence each other like natural rays if they originate from a beam originally polarized in a single direction.
5. In interference phenomena produced by rays that have undergone double refraction, the position of the fringes is not determined solely by the path difference and the difference of velocities; and in certain circumstances, which we have indicated, it is also necessary to take into account an additional difference equal to half a wavelength.

2.3. Mach-Zehnder interferometer

The Mach-Zehnder interferometer, proposed between 1981 and 1982 by Ludwig Mach and Ludwig Zehnder, is another amplitude-division device. It consists of two beam splitters and two fully reflective mirrors. The two waves inside the apparatus travel along separate paths; see Figure 1. A difference between the optical lengths of the paths can be introduced by slightly tilting one of the beam splitters. Because the two paths are separated, the interferometer is relatively difficult to align. However, for the same reason, the interferometer finds a wide range of applications. It has even been used, in a somewhat modified but conceptually similar form, to obtain electron interference fringes.

An object inserted into one of the beams alters the optical path length difference, thereby changing the fringe pattern. A common application of this device is to observe density variations in gas-flow patterns inside research chambers (wind tunnels, shock tubes, etc.).

2.4. Materials

The following materials were used to carry out the measurements and experiments:

- HeNe laser (15 mW, @632.5 nm)
- 4 mirrors
- 2 cube-type beam splitters
- 2 linear polarizers
- Power meter
- 1 $\lambda/2$ wave plate
- Mounts for optical elements
- Filter
- Camera

3. Procedure

In this practice, the Mach-Zehnder interferometer was built as illustrated in Figure 1, using the notation shown in the diagram to refer to the different analysis points. First, the alignment and collimation of a vertically polarized laser were performed. Next, the interferometer setup was configured as shown in Figure 2. Once the initial configuration was completed, four specific procedures were carried out.

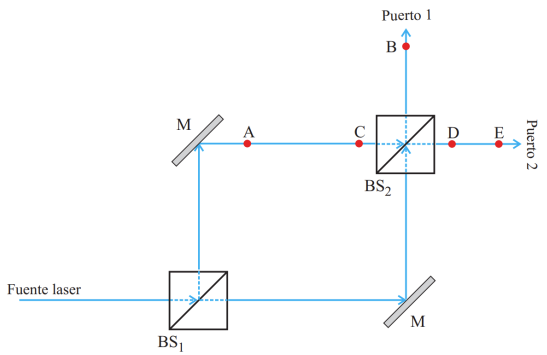


Figure 1. Mach-Zehnder interferometer diagram.

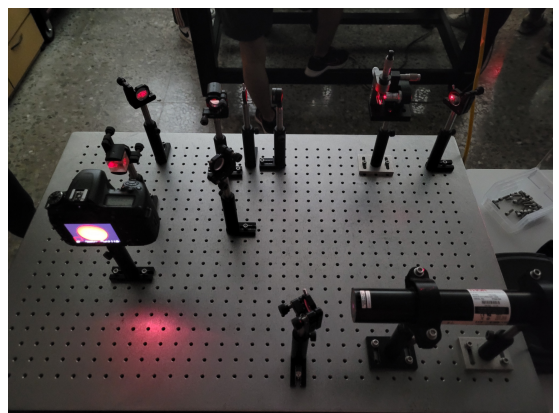


Figure 2. Experimental setup of the Mach-Zehnder interferometer.

In the first procedure, the natural behavior of the interference generated by the interferometer was examined. Since this device allows manipulation of independent optical paths, in the second procedure a filter was incorporated to analyze the generated interference fringes in greater detail. In the third procedure, the optical path length and the wavefront shape were changed. Finally, in the fourth procedure, configurations involving interference with different polarizations were explored. Each procedure was performed with the goal of gaining a deep understanding of the Mach-Zehnder interferometer behavior and its ability to generate and analyze optical interference under a variety of conditions and configurations, using the diagram notation for precise reference at each stage of the experiment.

3.1. Interference behavior

To study the interference behavior, the setup shown in Figure 2 was used. A precise alignment of the two output mirrors was carried out to ensure optimal initial conditions. Subsequently, a photograph of the generated pattern was captured without making any modifications to the setup, as shown in Figure 3.

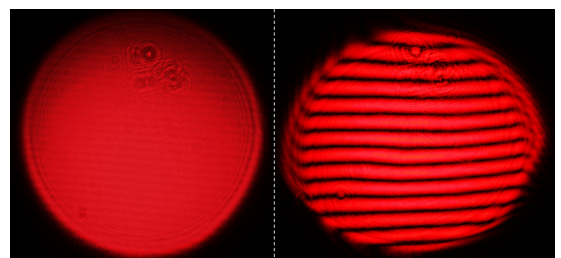


Figure 3. Pattern before alignment, and aligned pattern with interference.

In the next step, a lighter was introduced into one of the interferometer arms and changes in the interference pattern were observed,

as illustrated in Figure 4.

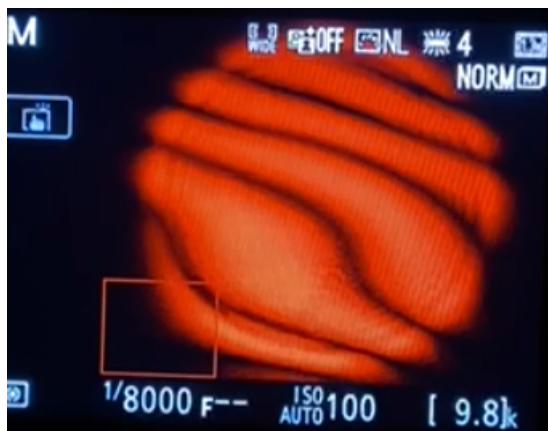


Figure 4. Deformations produced by a lighter placed in one arm.

Then, the effects of misaligning the mirrors on the fringe pattern were studied. The results of these changes are shown in Figure 5.

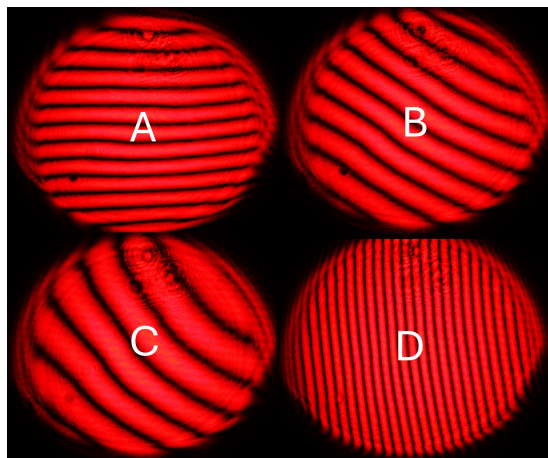


Figure 5. Images A–D show how the fringe pattern rotates and how the number of fringes changes in the interference.

It is important to note that the analysis and observations section will describe and explain the phenomena observed during these experiments.

3.2. Filter behavior

In this procedure, the pattern and intensity produced by the interference were analyzed. A neutral-density filter of 3 was introduced at the position labeled A in Figure 1, and the intensity in that same arm was measured with and without the filter to determine the percentage of light transmitted by the filter. Then, with the filter placed at position A, the contrast between fringes was observed and an image of the interference pattern was recorded. Figure 6 shows the intensity pattern obtained in this step.

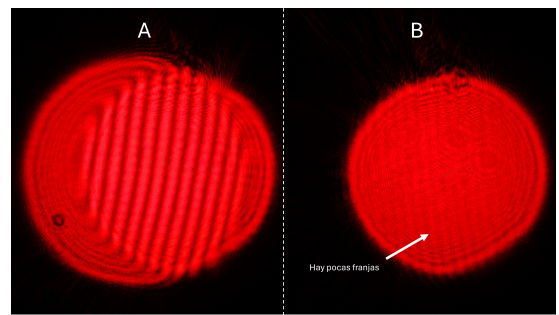


Figure 6. Image A: interference without filter. Image B: interference with a filter in one arm.

Once this part was completed, the filter was placed at the position labeled B and the fringe contrast was observed. The resulting intensity pattern is shown in Figure 7.

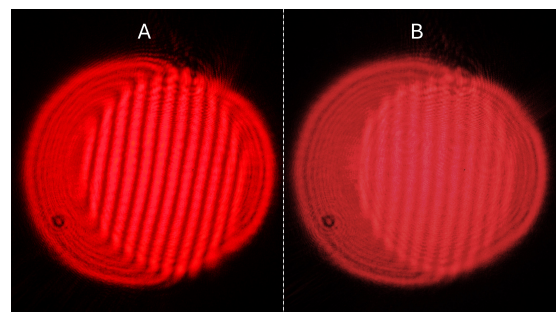


Figure 7. Image A: interference without filter. Image B: interference with a filter at the interferometer output.

3.3. Optical path and wavefront study

To study optical-path changes, the interferometer was aligned to produce only one fringe, then a glass plate was placed as shown in Figure 8. Subsequently, interference patterns were observed while rotating the glass plate, which increased the optical path in that arm, as visualized in Figure 9.



Figure 8. Experimental setup with a glass plate modifying the optical path.

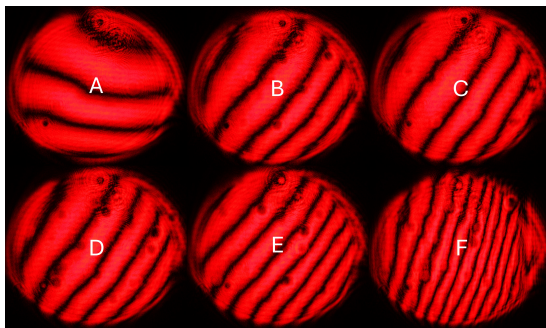


Figure 9. Images A–F show how the interference pattern changes as the glass plate is gradually rotated.

In another procedure, interference between a plane wave and a spherical wave was analyzed. For this, a biconvex lens (the specific lens type was not critical) was introduced in one arm of the interferometer, producing a spherical wavefront. Since the beam in the other arm was already collimated, producing a plane wavefront, the resulting interference pattern could be observed, as shown in Figure 10.

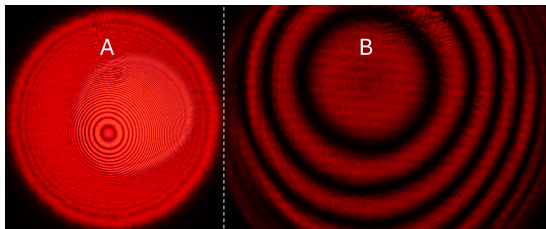


Figure 10. Image A shows annular interference. In image B, the same is performed, but the number of rings is reduced to improve visualization.

3.4. Polarization study

In this procedure, a $\lambda/2$ wave plate was placed in arm A of the interferometer so that rotating it would change the initial vertical polarization into a different direction. The wave plate was rotated until reaching 45 degrees with respect to the fast axis, which resulted in the disappearance of the interference, as shown in Figure 11 (it is important to recall that at 45 degrees one obtains polarization).

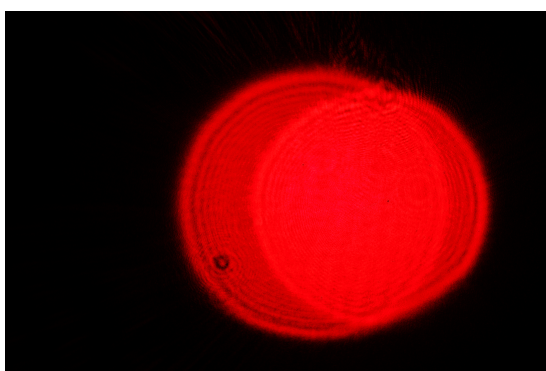


Figure 11. Two fields with different polarizations superposed, but without interference.

Subsequently, a linear polarizer was placed at output A of the interferometer and rotated until achieving the highest fringe intensity, as illustrated in Figure 12. The polarizer was positioned at 45 degrees relative to the vertical axis for this step.

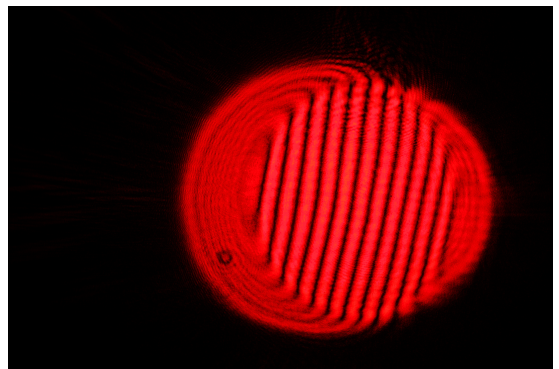


Figure 12. Two fields with different polarizations superposed, but with interference recovered by a linear polarizer.

4. Analysis and Observations

4.1. Interferometer behavior

The Mach-Zehnder interferometer enabled the separation of two independent light paths, which facilitated the study of optical interference. However, a high sensitivity to environmental changes was observed; even small vibrations or taps on the table resulted in visible deformations in the interference fringes.

4.1.1. Interference formation and fringes

During the experiment, the formation of interference patterns and alternating intensity fringes was clearly observed. Mirror motion produced variations in the interference due to displacement between the two generated fields. Through experimental study with plane waves, a relationship between field displacement and the orientation and number of fringes was established, as illustrated in Figure 13.

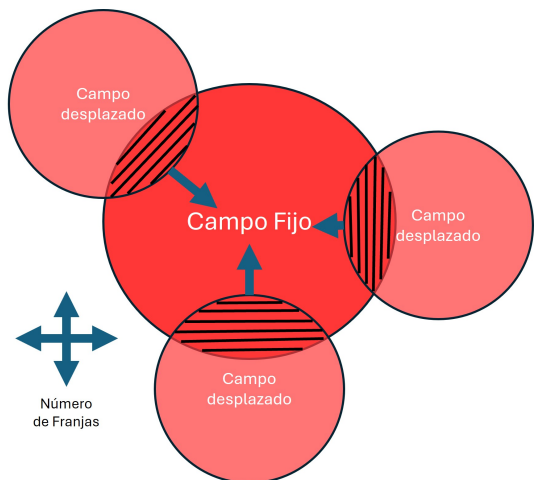


Figure 13. Diagram of fringe distribution as a function of the displacement of the interfering fields.

As can be seen, the orientation of the fringes depends on the interference region: whether the fields overlap top-to-bottom, left-to-right, or laterally with a certain tilt. Meanwhile, the number of fringes depends on the displacement itself, regardless of where it starts, and when both fields are perfectly aligned, the fringes disappear. This information is crucial for understanding the wave shape and will be useful in modulated fringe projection.

4.1.2. Temperature influence

Based on what is observed in Figure 4, variations in air temperature were shown to impact the density and refractivity of the medium, producing irregular changes in the optical path. This, in turn, affected the sharpness and position of the interference fringes. These findings highlight the critical importance of maintaining stable environmental

conditions during measurements to ensure precise and consistent results.

4.1.3. Optical-path influence

Changes in the optical-path length in the interferometer, through the glass plate placed in one arm as shown in Figure 9, resulted in significant changes in the interference pattern. By modifying the length of one path, both the number and orientation of the interference fringes were affected. This suggests a diagonal shift in the interference pattern, as illustrated in Figure 14. This occurs because the fringes changed from horizontal to vertical.

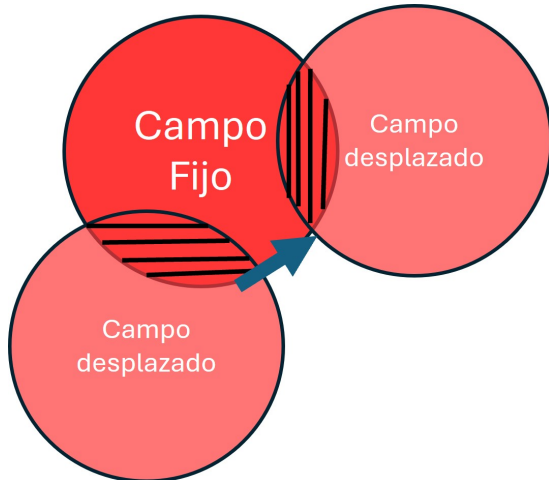


Figure 14. Diagram of the interference change when the optical path is modified by rotating a glass plate.

4.2. Modifications to the interferometer arms

During the experiment, several modifications were performed on the interferometer arms to study different optical phenomena. Each observed phenomenon is described below.

4.2.1. Attenuation with filters

Introducing neutral-density filters in one arm of the interferometer allowed control of the incident light intensity and the study of how this affected the interference pattern. An ND = 3.0 filter was used, which implies a transmission of only 0.1% of the intensity. However, when analyzing the intensity observed in Figure 6 using Matlab, the transmitted light was found to be 5.9026%. This suggests a considerable discrepancy in the filter behavior, possibly due to a residual contribution from the unfiltered field, which adds to this percentage.

Although the filtered field is no longer visible to the naked eye, a faint set of fringes can still be observed, indicating that a small amount of filtered light remains present in the configuration.

In the case of Figure 7, where the filter was placed at the interferometer output, only a reduction in overall intensity was observed, which is expected since no field was modified.

4.2.2. Polarization

By modifying the polarization of the incident light using wave plates and polarizers, we explored how polarization affects interference and the observed fringes. In Figure 11, it is shown that when the superposed fields have different polarizations (one vertical and one horizontal generated with a $\lambda/2$ wave plate at 45 degrees), no interference is present. However, by adding a linear polarizer at 45 degrees, the two different polarizations become diagonal, allowing interference to be recovered, as shown in Figure 12.

Interference of electric fields is essentially a vector sum. Two vectors add up to a zero vector if, and only if, they are anti-collinear and have the same magnitude.

The (anti)collinearity condition is achieved only in special cases. One such case is linearly polarized waves with the same polarization (they must also propagate under a similar angle for good fringe contrast; otherwise, the vectors are no longer collinear).

If the field vectors are not collinear, as in waves with different polarizations, they can never subtract to yield zero.

Suppose now that we have two real vector fields $\mathbf{E}_1, \mathbf{E}_2$. The (instantaneous) intensity of each field is (up to a constant factor) given by $\mathbf{E}_1 \cdot \mathbf{E}_1, \mathbf{E}_2 \cdot \mathbf{E}_2$.

If the two fields interfere, the instantaneous intensity is $(\mathbf{E}_1 + \mathbf{E}_2) \cdot (\mathbf{E}_1 + \mathbf{E}_2) = \mathbf{E}_1 \cdot \mathbf{E}_1 + \mathbf{E}_2 \cdot \mathbf{E}_2 + 2\mathbf{E}_1 \cdot \mathbf{E}_2$, where $2\mathbf{E}_1 \cdot \mathbf{E}_2$ is the interference term. Suppose that the polarization of \mathbf{E}_1 is orthogonal to the polarization of \mathbf{E}_2 , for example:

$$\mathbf{E}_1 = \begin{pmatrix} E_{1x} \\ 0 \\ 0 \end{pmatrix}, \quad \mathbf{E}_2 = \begin{pmatrix} 0 \\ E_{2y} \\ 0 \end{pmatrix}$$

Then, $\mathbf{E}_1 \cdot \mathbf{E}_2 = 0$, which means the two fields cannot interfere. This observation is the First Fresnel–Arago Law: fields with orthogonal polarization cannot interfere.

4.2.3. Wavefront modification

Introducing optical elements to modify the wavefront, such as a bi-convex lens, allowed us to study how wavefront curvature influences the formation of interference patterns. The results in Figure 10 are consistent with the theoretical interference pattern; see Figure 15.

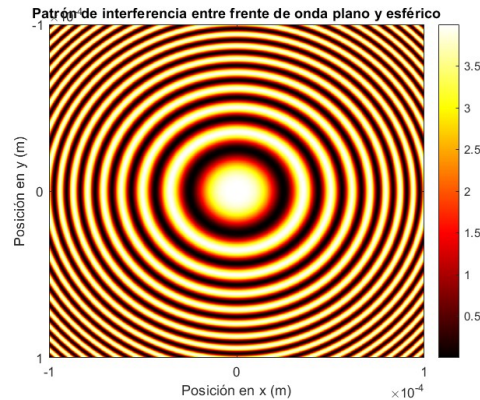


Figure 15. Interference pattern between a plane wavefront and a spherical wavefront.

These results highlight the versatility of the Mach-Zehnder interferometer to study a broad range of optical phenomena and the importance of considering different variables in the experimental configuration to obtain precise and meaningful results.

5. Conclusions

This laboratory experience has been fundamental for my professional development in optics and optical interference. Through the detailed exploration and analysis of the optical phenomena associated with the Mach-Zehnder interferometer, I deepened my understanding of light interference, polarization, and interferometric sensitivity. Careful calibration of optical components, such as polarizers and wave plates, was essential at each experimental stage, underscoring the importance of precision in the alignment of the elements.

A notable aspect of this practice was the correlation between experimental results and theoretical predictions, supported by simulations in MATLAB. This not only validated the concepts learned in class, but also demonstrated the usefulness of computational tools in optical research.

I learned significantly about the importance of meticulous planning and careful execution in experimentation. Each step, from alignment of elements to manipulation of polarization and wavefronts,

influenced the final results. This experience strengthened my ability to approach scientific challenges with rigor and precision, preparing me for future projects in experimental optics and research.

In summary, this practice not only expanded my theoretical understanding of optical phenomena, but also improved my practical skills and methodological approach in the laboratory, providing a solid foundation for future studies and scientific contributions. In the future I hope to work in nuclear fusion; I am confident that this knowledge in optics will be key to my professional development.

6. Appendices

Appendices (SharePoint folder)

7. References

1. Arago, F., & Fresnel, A. J. (1819). Mémoire sur l'action que les rayons de lumière polarisés exercent les uns sur les autres. De l'Imprimerie de Feugueray, rue du Cloître Saint-Benoit, no. 4.
2. Arteaga, O. (2021). Fresnel-Arago fifth law of interference: the first description of a geometric phase in optics. *Journal of Modern Optics*, 68(6), 350–356. <https://doi.org/10.1080/09500340.2021.1898687>
3. Hecht, E. (2022). Optics (5th ed.). Pearson. ISBN 978-1-292-09693-3.
4. Konijnenberg, S., Adam, A. J. L., & Urbach, H. P. (2024). OPTICS. Delft University of Technology. Retrieved from LibreTexts website: <https://libretexts.org>
5. Morales Durán, N., & Gutiérrez López, L. A. (2014, May 10). Interferómetro de Mach-Zehnder. Universidad de los Andes, Departamento de Física.

Juan Pablo Solís Ruiz - A01067387

Contact:

 A01067387@tec.mx